J|A|C|S
ARTICLES
Published on Web 06/14/2002

A ^{13}C INADEQUATE and HF-GIAO Study of $C_{60}H_2$ and $C_{60}H_6$ Identification of Ring Currents in a 1,2-Dihydrofullerene

Mark S. Meier,*[,†,§] H. Peter Spielmann,*[,†,‡] Robert G. Bergosh,[†,§] and Robert C. Haddon*[,§,⊥]

Contribution from the Department of Chemistry, Department of Molecular and Cellular Biochemistry, and Advanced Carbon Materials Center, The University of Kentucky, Lexington, Kentucky 40506-0055, and the Department of Chemistry, University of California, Riverside, California 92521-0403

Received November 8, 2001. Revised Manuscript Received April 10, 2002

Abstract: The hydrofullerenes $C_{60}H_2$ (**1**) and $C_{60}H_6$ (**2**) have been prepared in ^{13}C-enriched form and 2D INADEQUATE NMR spectra were measured. These spectra have provided unambiguous ^{13}C assignments for **2**, and nearly unambiguous assignments for **1**. In both cases, the most downfield resonances are immediately adjacent to the sp^3 carbons, despite the fact that these carbons are the least pyramidalized carbons in the molecule. Typically, ^{13}C chemical shifts move downfield with increasing pyramidalization (Θ_p), but in these systems there is no strong correlation between Θ_p and δ. HF-GIAO calculations are able to predict the chemical shifts, but provide little chemical insight into the origin of these chemical shifts. London theory reveals a significant paramagnetic ring current in **1**, a feature that helps explain the ^1H shifts in these compounds and may contribute to the ^{13}C chemical shifts as well.

NMR chemical shifts contain a great deal of information about the electronic structure of molecules.[1] The primary tool for establishing structure in fullerene chemistry is ^{13}C NMR. However, ^{13}C NMR is often only used to establish the symmetry of a new fullerene derivative due to complexity of the spectra and the inherently low sensitivity of the method. The poor understanding of chemical shift dispersion in fullerenes prevents the effective use of the additional information present in the absolute chemical shifts.

There has been no systematic study in which complete chemical shift assignments have been analyzed with a view toward identifying the structural origin of the chemical shifts and using the assignments to predict reactivity in fullerenes. The literature contains relatively few examples of complete assignments of ^{13}C NMR resonances in fullerene derivatives, and complete assignments are the starting point for any study to correlate chemical shifts with reactive sites. 2D INADEQUATE NMR spectroscopy was used to assign the ^{13}C spectrum of a C_{60}-osmium tetraoxide adduct,[2] a Hirsch−Bingel adduct,[3] and a tethered fullerene bisadduct,[4] and was also used in the assignment of unusual 1,16 regiochemistry resulting from radical addition to C_{60}.[5] The chemical shifts of the 5 different carbons in C_{70} were assigned using 2D INADEQUATE NMR spectroscopy based on relative intensities and carbon connectivity,[6] and also using pyramidalization, with the most downfield resonances being assigned to the most pyramidalized carbons in the molecule.[7,8] INADEQUATE experiments have also been used to help determine the structures of a set of C_{60} and C_{70} cyclopropanes and fulleroids[9] and a 1,4 bisgermylated cycloadduct of C_{60}.[10] In addition, heteronuclear coupling constants can be used to assign resonances. Some ^{13}C resonances in $(C_{59}N)_2$ were assigned through $^{15}N-^{13}C$ coupling constants,[11] and our group has assigned some ^{13}C resonances in $C_{60}H_n$ and $C_{70}H_n$ species through the use of $^1H-^{13}C$ coupling constants.[12−15]

We report full assignment of the ^{13}C NMR resonances of the C_{60} derivatives 1,2-$C_{60}H_2$ (**1**) and 1,2,33,41,42,50-$C_{60}H_6$ (**2**),

* Corresponding author. E-mail: meier@pop.uky.edu.
† Department of Chemistry, The University of Kentucky.
§ Advanced Carbon Materials Center, The University of Kentucky.
‡ Department of Molecular and Cellular Biochemistry, The University of Kentucky.
⊥ Department of Chemistry, University of California.

(1) Jameson, C. J. *Annu. Rev. Phys. Chem.* **1996**, *47*, 135−169.
(2) Hawkins, J. M. *Acc. Chem. Res.* **1992**, *25*, 150−156.
(3) Burley, G. A.; Keller, P. A.; Pyne, S. G.; Ball, G. E. *Magn. Reson. Chem.* **2001**, *39*, 466−470.
(4) Burley, G. A.; Keller, P. A.; Pyne, S. G.; Ball, G. E. *Chem. Commun.* **2000**, 1717−1718.
(5) Ford, W. T.; Nishioka, T.; Qiu, F.; D'Souza, F.; Choi, J.-P. *J. Org. Chem.* **2000**, *65*, 5780−5784.
(6) Johnson, R. D.; Meijer, G.; Salem, J. R.; Bethune, D. S. *J. Am. Chem. Soc.* **1991**, *113*, 3619−3621.
(7) Johnson, R. D.; Bethune, D. S.; Yannoni, C. S. *Acc. Chem. Res.* **1992**, *25*, 169−175.
(8) Taylor, R.; Hare, J. P.; Abdul-Sada, A. D.; Kroto, H. W. *J. Chem. Soc., Chem. Commun.* **1990**, 1423−1424.
(9) Smith, A. B., III; Strongin, R. M.; Brard, L.; Furst, G. T.; Romanow, W. J.; Owens, K. G.; Goldschmidt, R. J.; King, R. C. *J. Am. Chem. Soc.* **1995**, *117*, 5492−5502.
(10) Akasaka, T.; Wakahara, T.; Mizushima, T.; Ando, W.; Walchli, M.; Suzuki, T.; Kobayashi, K.; Nagase, S.; Kako, M.; Nakadaira, Y.; Fujitsuka, M.; Ito, O.; Sasaki, Y.; Yamamoto, K.; Erata, T. *Org. Lett.* **2000**, *2*, 2671−2674.
(11) Belavia-Lund, C.; Keshavarz-K., M.; Collins, T.; Wudl, F. *J. Am. Chem. Soc.* **1997**, *119*, 8101−8102.
(12) Meier, M. S.; Weedon, B. R.; Spielmann, H. P. *J. Am. Chem. Soc.* **1996**, *118*, 11682−11683.
(13) Bergosh, R. G.; Laske Cooke, J. A.; Meier, M. S.; Spielmann, H. P.; Weedon, B. R. *J. Org. Chem.* **1997**, *62*, 7667−7672.
(14) Spielmann, H. P.; Wang, G.-W.; Meier, M. S.; Weedon, B. R. *J. Org. Chem.* **1998**, *9865*, 5−9871.
(15) Weedon, B. R.; Haddon, R. C.; Meier, M. S.; Spielmann, H. P. *J. Am. Chem. Soc.* **1999**, *335*, 5−340.

10.1021/ja012513r CCC: $22.00

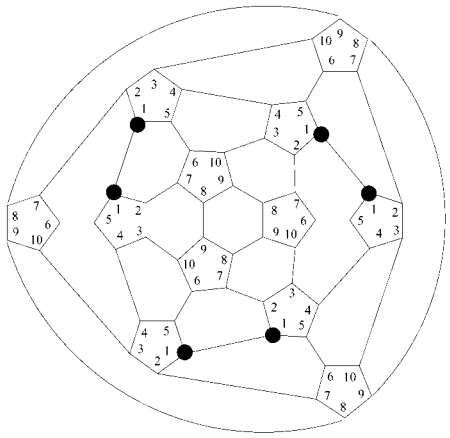

Figure 1. Planar projection of **2**, with chemically equivalent carbons labeled. The filled circles represent protonated sp^3 carbons.

as well as HF-GIAO calculations of those chemical shifts. We also discuss insights into the origin of the ^{13}C chemical shifts and the $^{13}C-^{13}C$ coupling constants.

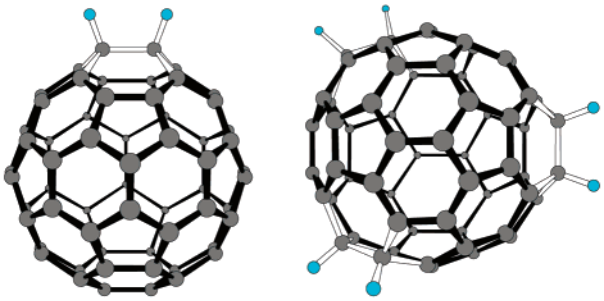

1 **2**

The high (D_3) symmetry of **2** leads to only 10 different carbon resonances, with one of those being due to a unique sp^3 carbon and nine resonances due to sp^2 carbons. We have previously assigned the resonances that are the most downfield in CS_2 solution (158.05 and 153.97 ppm[12]) as the sp^2 carbons that are closest to the sp^3 carbon, using ^1H-coupled ^{13}C NMR. These particular sp^2 carbons are labeled "2" and "5" in Figure 1. The ^1H coupling diminishes rapidly with distance in **2**, so it was not possible to make any additional assignments.

By using the 51.47 ppm sp^3 resonance as a starting point, the carbon−carbon connectivity of **2** was easily determined from the INADEQUATE spectrum. The assignments are shown in Figure 2. There is a small solvent effect on the chemical shifts, as in ODCB the third most downfield resonance (152.97 ppm) is adjacent to a protonated carbon, while the second most downfield resonance (153.15 ppm) is not, a different arrangement from what was observed in CS_2 solution.[12]

There is a nearly perfect segregation of chemical shifts in **2**. The most downfield chemical shifts (in the 150−160 ppm range) are due to the carbons in a pentagon containing a sp^3 carbon atom, and the upfield chemical shifts (in the 140−150 ppm range) are due to carbons in a pentagon composed entirely of sp^2 carbon atoms.

When C_{60} reacts to form the C_{2v} structure of **1**, the single chemical shift of C_{60} (143 ppm) converts to a set of resonances composed of one sp^3 resonance at 54.10 ppm and a set of 16 sp^2 resonances that span nearly 20 ppm, from an upfield

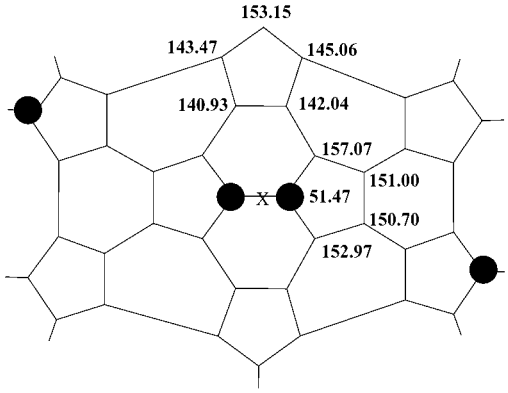

Figure 2. Partial structure of **2**, showing the 10 unique carbon atoms and chemical shifts. The X denotes a C_2 symmetry axis. The dark circles denote protonated sp^3 carbon atoms.

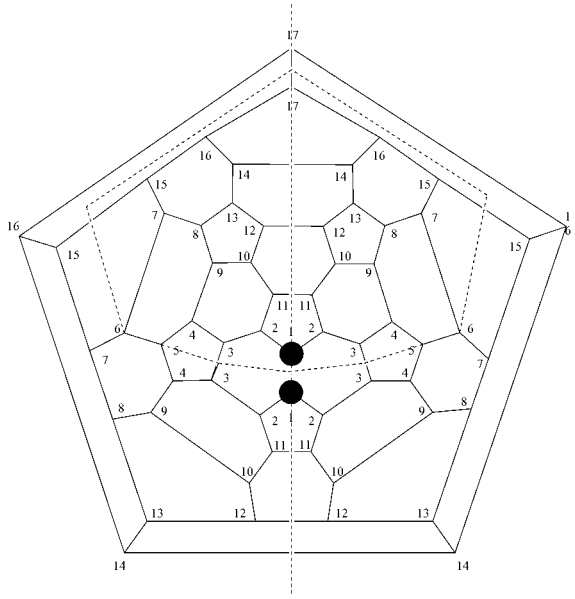

Figure 3. Projection of $C_{60}H_2$, showing the planes of symmetry (dashed lines) and identifying the chemically equivalent carbons. The filled circles represent the protonated carbons.

resonance at 136.50 ppm to a downfield resonance at 152.69 ppm (in ODCB-d_4). Clearly the 20 ppm dispersion of sp^2 chemical shifts reflects changes in structure and in the electronic environment at different atoms that may also be manifest in different reactivity, although this relationship is not simple.

The C_{2v} structure of **1** has 4 identical quadrants (see Figure 3) with 17 inequivalent carbon atoms that produce the 17 ^{13}C chemical shifts listed in Table 1. The single sp^3 resonance at 54.10 ppm (ODCB-d_4) is easily assigned to the chemically equivalent sp^3 carbons C1 and C2, leaving 16 sp^2 resonances to be assigned through the INADEQUATE experiment. The 2-bond $^1H-^{13}C$ couplings previously[13] allowed us to assign the resonance that is the most downfield (152.69 ppm) as resulting from the sp^2 carbons closest to the sp^3 carbons (labeled as "1" in Figure 3), and this is confirmed by the INADEQUATE experiment in ODCB. This is also the pattern observed in $C_{60}(C(CO_2H))_2$.[3]

Complete assignment of the ^{13}C resonances of **1** was a challenge, as several resonances were nearly coincident, even at a spectral frequency of 125 MHz. The close, 0.02 ppm (2.5 Hz) spacing of the resonances at 142.17 and 142.19 ppm leads

Table 1. Experimental and Calculated Chemical Shifts in **1**

carbon label[a]	rel intensity	exptl chemical shift	HF-GIAO chemical shift[c]
1	2	53	41.1
2	4	152.69	148.2
3	4	136.56	133.3
4	4	142.19[b]	142.5
5	2	146.33	145.9
6	2	143.53	145.0
7	4	146.61	145.8
8	4	144.94	145.0
9	4	145.72	144.8
10	4	140.59	140.9
11	4	148.00	146.9
12	4	141.81	142.1
13	4	142.17[b]	142.4
14	4	142.76	142.9
15	4	145.65	145.0
16	4	146.54	145.5
17	2	147.61	146.7

[a] Carbon labels from Figure 2. [b] These may be reversed. See text. [c] Chemical shifts were normalized to the calculated chemical shift for benzene, assigned to 122 ppm.

to both of these resonances showing several of the same correlations to other carbon atoms. The assignments of the resonances (Table 1) are the most consistent with the data.

With assignments completed, we were able to examine the structural features that contribute to the various chemical shifts. Several patterns, common to both **1** and **2**, were noticed immediately. First, in both molecules studied, the most downfield resonances are due to carbons that are immediately adjacent to the sp^3 carbons. This appears to also be the case with the cyclopropane $C_{61}H_2$.[9] Second, the most upfield resonances are due to carbons that are immediately adjacent to the carbons that are most downfield. The rest of the chemical shifts are fairly closely spaced, which is not unexpected given the very similar chemical and electronic environments of many of the carbons located far from the site of reaction.

We have examined several quantifiable structural features in an effort to uncover the origin of the chemical shift dispersion in **1** and **2**. Since crystal structures are not available for these compounds, we calculated the structures of **1** and **2** at the B3LYP/6-31G* level of theory. Since chemical shift calculations are very sensitive to the geometry,[16] it was important to validate the calculated structure with experimental data. To address the quality of the calculated structure, we compared measured coupling constants ($^1J_{CC}$) extracted from 2-dimensional INADEQUATE[17] ^{13}C NMR spectra performed on 13% ^{13}C enriched samples **1** and **2** with the bond lengths from the calculated structure. The measured coupling constants are directly proportional to the C−C bond lengths. A smaller coupling constant indicates that a bond is long, and therefore has more single bond character, while a large coupling constant indicates a short bond, and therefore more double bond character.

The coupling constants between carbons along 5−6 ring fusions range from 52 to 58 Hz, and those for the 6−6 ring fusions ranged from 66 to 71 Hz. The measured coupling constants indicate that the 6−6 ring fusion bonds are shorter than the 5−6 ring fusion bonds, consistent with the pattern seen in C_{60} itself.[18]

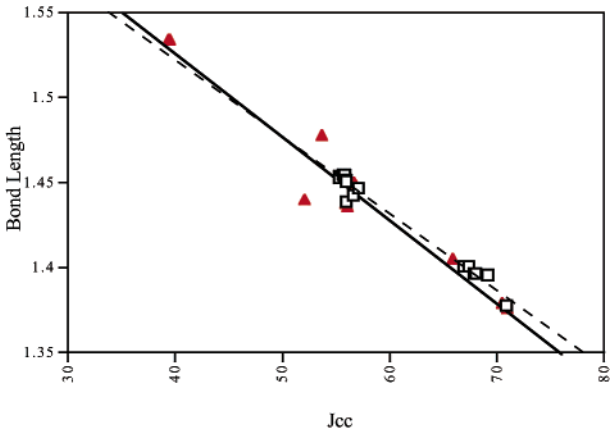

Figure 4. Correlation of measured C−C coupling constants with calculated C−C bond lengths for **1** (squares) and **2** (triangles). The lines shown are linear regression fits: dashed line, **1**; solid line, **2**.

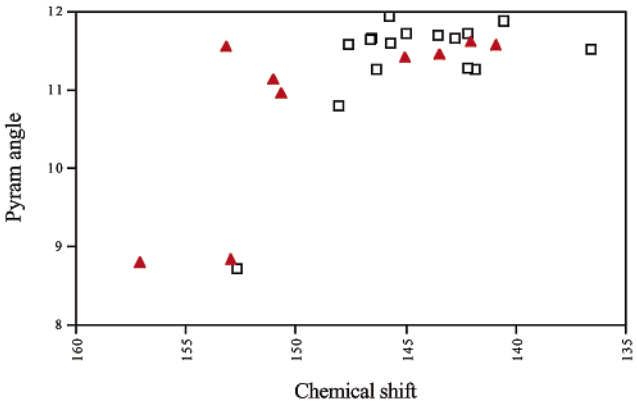

Figure 5. Plot of pyramidalization angle (θ_p) versus the experimental ^{13}C chemical shift in **1** (squares) and in **2** (triangles).

The one-bond carbon−carbon coupling constants in **1** and **2** are correlated with calculated bond lengths with r^2 values of 0.980 and 0.947, as shown in Figure 4. The quality of the linear correlation between the calculated structure and the measured coupling constants gives us confidence that the calculated structures are accurate.

The pyramidalization angle[19] (θ_p) of sp^2 carbons correlates well with chemical shifts in C_{70},[19] with the chemical shifts of some bowl-shaped hydrocarbons,[20,21] and has been used to rationalize the spread of chemical shifts in different isomers of C_{84}.[16,22] Plots of θ_p vs δ for both **1** and **2** (Figure 5) reveal that there is no strong trend in these cases. In fact, the least pyramidalized carbons are the most downfield, contrary to the trend seen in C_{70}. While s-character (as measured by θ_p) may be involved in the determination of the chemical shift of these carbon atoms, it is clearly not the sole factor.

We calculated the chemical shifts using HF-GIAO theory to see if these chemical shifts could be modeled computationally. There have been several reports of the calculation of ^{13}C NMR chemical shifts[23] of fullerenes[22,24−29] and fullerene derivatives.[9,16,30−33] In some cases the agreement with experimental

(16) Heine, T.; Seifert, G.; Fowler, P. W.; Zerbetto, F. *J. Phys. Chem.* **1999**, *103*, 8738−8746.
(17) Buddrus, J. In *Encyclopedia of Magnetic Resonance*; Wiley, New York, 1996, pp 2491−2500.
(18) David, W. I. F.; Ibberson, R. M.; Matthewman, J. C.; Prassides, K.; Dennis, T. J. S.; Hare, J. P.; Kroto, H. W.; Taylor, R.; Walton, D. R. M. *Nature* **1991**, *353*, 147−149.
(19) Haddon, R. C.; Scott, L. T. *Pure Appl. Chem.* **1986**, *58*, 137−142.
(20) Schulman, J. M.; Disch, R. L. *J. Comput. Chem.* **1998**, *19*, 189−194.
(21) Ferrer, S. M.; Molina, J. M. *J. Comput. Chem.* **1999**, *20*, 1412−1421.
(22) Schneider, A.; Richard, S.; Kappes, M. M.; Ahlrichs, R. *Chem. Phys. Lett.* **1993**, *1993*, 165−169.

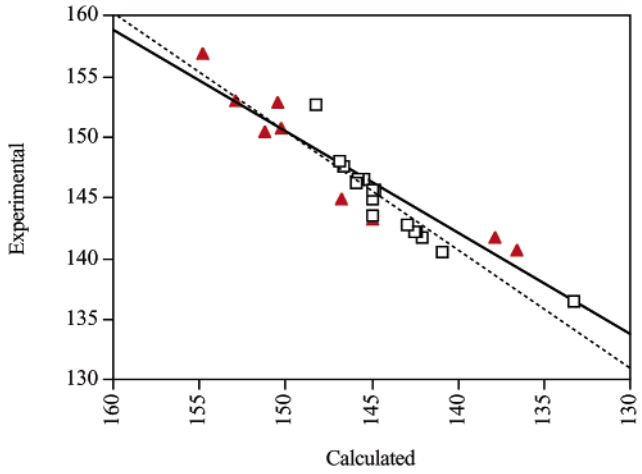

Figure 6. Experimental versus calculated chemical shifts for **1** (squares) and **2** (triangles). The lines shown are linear regression fits: dashed line, **1**; solid line, **2**.

chemical shifts has been good enough to assist with structural assignments of fullerene derivatives. In an effort to determine if computational methods can produce good agreement with the observed spectrum, the chemical shifts for **2** were calculated with HF-GIAO methods[1] using a B3LYP/6-31G* geometry, and referenced to benzene calculated in the same manner. The range of sp^2 chemical shifts (16 ppm) calculated by this method almost perfectly matches the observed range (16.1 ppm). All of the calculated chemical shifts are within ca. 2 ppm of the experimental values, except for resonances due to carbons labeled as "6" and "7" in Figure 1. The agreement with the observed values is good ($r^2 = 0.879$) (Figure 6).

The observed chemical shifts of the ^{13}C resonances in **2** vary somewhat with the NMR solvent chosen, which complicates the issue of choosing an appropriate standard (see above).

Accurate calculation of the chemical shifts in **1** is somewhat more of a challenge, since there are more chemical shifts to contend with, plus many of these are more closely spaced than in **2**. By using the same computational methods described above, the chemical shifts for the carbon atoms in **1** were calculated and are shown in Table 1. Despite the increased complexity of this system, the overall agreement of theory with experiment ($r^2 = 0.847$) is similar to the agreement achieved with **2**. The calculated chemical shifts are offset slightly farther downfield than the experimental.

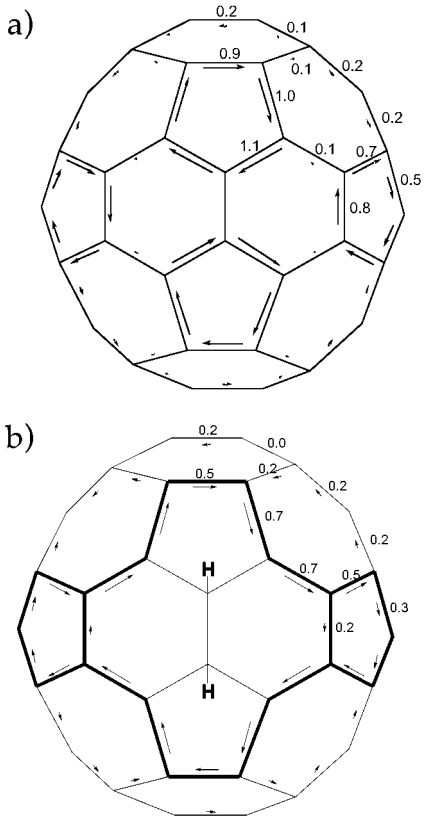

Figure 7. Electron ring currents in (a) C_{60} and (b) **1** for a magnetic field perpendicular to the projection of the molecule as shown on the page. The currents strength is given in units of the value for benzene. The dark lines in part b indicate the macrocyclic ring current.

The chemical shift calculations do not themselves provide "chemical insight" into the origin of the chemical shifts. In an effort to understand the changes in the electronic structure of these aromatic compounds, we investigated changes in the ring currents that are induced by hydrogenation. Hydrogenation of a C=C bond in C_{60} results in a "hole" in an otherwise spherical π-cloud[34] that had formerly carried both diamagnetic and paramagnetic ring currents.[35] The net effect of these currents is that the carbon resonance in C_{60} appears at 143 ppm.[36] Reduction of a C=C bond alters this uniform pattern. We speculated that reduction of a C=C bond forces a paramagnetic ring current to circulate around the perimeter of an annulene surrounding the sp^3 carbons (Figure 7), and that this ring current generates a field that affects chemical shifts. Calculations with the London methodology that we used on the fullerenes[36] show that a significant paramagnetic ring current circulates around a [12]annulene.[37,38] The ring current bifurcates at two points, with significant current moving into peripheral five-membered rings,

(23) For an issue of *J. Comput. Chem.* devoted to the calculation of NMR and EPR parameters, see: *J. Comput. Chem.* **1999**, *20* (12), 1199−1327.
(24) Heine, T.; Zerbetto, F.; Seifert, G.; Fowler, P. W. *J. Phys. Chem. A* **2000**, *104*, 3865−3868.
(25) Heine, T.; Buhl, M.; Fowler, P. W.; Seifert, G. *Chem. Phys. Lett.* **2000**, *316*, 373−380.
(26) Bühl, M.; Kaupp, M.; Malkina, O. L.; Malkin, V. G. *J. Comput. Chem.* **1999**, *20*, 91−105.
(27) Grossman, J. C.; Cote, M.; Louie, S. G.; Cohen, M. L. *Chem. Phys. Lett.* **1998**, *284*, 344−349.
(28) Baker, J.; Fowler, P. W.; Lazzeretti, P.; Malagoli, M.; Zanasi, R. *Chem. Phys. Lett.* **1991**, *184*, 182−186.
(29) Fowler, P. W.; Lazzeretti, P.; Malagoli, M.; Zanasi, R. *J. Phys. Chem.* **1991**, *95*, 6404−6405.
(30) Kitagawa, T.; Sakamoto, H.; Takeuchi, K. *J. Am. Chem. Soc.* **1999**, *121*, 4398−4399.
(31) Sato, N.; Tou, H.; Maniwa, Y.; Kikuchi, K.; Suzuki, S.; Achiba, Y.; Kosaka, M.; Tanigaki, K. *Phys. Rev. B: Condens. Matter Mater. Phys.* **1998**, *58*, 12433−12440.
(32) Bühl, M.; Curoni, A.; Andreoni, W. *Chem. Phys. Lett.* **1997**, *274*, 231−234.
(33) Laali, K. K.; Hollenstein, S.; Galembeck, S. E.; Nakamura, Y.; Nishimura, J. *J. Chem. Soc., Perkin Trans. 2* **1999**, 2129−2132.
(34) For a recent review article on aromaticity of fullerenes, see: Bühl, M.; Hirsch, A. *Chem. Rev.* **2001**, *101*, 1153−1183.
(35) Haddon, R. C.; Schneemeyer, L. F.; Waszcak, J. V.; Glarum, S. H.; Tycko, R.; Dabbagh, G.; Kortan, A. R.; Muller, A. J.; Mujsce, A. M.; Rosseinsky, M. J.; Zahurak, S. M.; Makhija, A. V.; Thiel, F. A.; Raghavachari, K.; Cockayne, E.; Elser, V. *Nature* **1991**, *350*, 46−47.
(36) Pasquarello, A.; Schlüter, M.; Haddon, R. C. *Phys. Rev. A* **1993**, *47*, 1783−1789.
(37) For a different approach to the calculation of ring currents in annulenes that illustrate macrocyclic ring currents, see: Steiner, E.; Fowler, P. W.; Jenneskens, L. W. *Angew. Chem., Int. Ed. Engl.* **2001**, *40*, 362−366 and references therein.

increasing the paramagnetic ring size up to an [18]annulene. The magnitudes and paths of the ring currents are shown in Figure 7a,b.

Experimental evidence for this ring current includes the significant downfield ^{1}H chemical shift of the protons in $C_{60}H_2$ (7.17 ppm in CS_2),[13] consistent with the protons being positioned within a strong paramagnetic ring current. This ring current may affect the chemical shift of the adjacent carbons.

The high-field sp^2 carbon "3" resonates at 136.56 ppm (Figure 2), 7 ppm upfield of the average for the molecule, which may be due in part to the effect of this ring current. Carbon "2" (Figure 2, the only carbon at the junction of the macrocyclic ring and one diamagnetic ring) and carbon "11" appear shifted significantly downfield (152.69, 148.00 ppm, respectively).

Conclusions

The ^{13}C NMR spectra of 1,2-$C_{60}H_2$ (**1**) and 1,2,33,41,42,50-$C_{60}H_6$ (**2**) have been measured and assigned with use of 2D INADEQUATE methodology. In both cases, the most downfield resonances are due to sp^2 carbons immediately adjacent to the sp^3 carbons. Interestingly, the most upfield resonances are due to carbons that are adjacent to the most downfield carbons. The appearance of a new pattern of ring currents in the reduced compounds may be involved in these downfield shifts. Pyramidalization angles correlate only roughly with the chemical shift, in contrast to the good correlation seen in C_{70}. Chemical shifts calculated with HF-GIAO methods starting from DFT-derived structures agree reasonably well with the observed chemical shifts, but the theory does not appear to be able to fully account for the magnetic environment present in the electronic structure of these spherical aromatic systems.

Experimental Section

Fullerenes. Samples of ^{13}C-enriched $C_{60}H_2$ and $C_{60}H_6$ were prepared from 13% ^{13}C-enriched C_{60} (MER Corp.) by the standard Zn/Cu method.[13] Saturated, FPT-deoxygenated solutions of these samples in 1,2-dichlorobenzene-d_4 were sealed under vacuum in 5 mm NMR tubes. All 2D INADEQUATE ^{13}C experiments were recorded at 25 °C at 125.7 MHz on a Varian Inova spectrometer with a spectral width (for **1**) of 14814.8 Hz and 32 768 real points in ω_2, and (for **2**) a spectral width of 2 482 Hz and 16 384 real points in ω_2. One-bond C−C coupling constants were extracted from the INADEQUATE spectrum and correlated resonances were identified with the aid of the digital signal processing program FRED (Varian), with a resolution of 0.15 (for **1**) or 0.45 Hz (for **2**). Digital oversampling by a factor of 15 (for **1**) was employed to reduce baseline distortions associated with the spectrometer's low-pass filters.[39] All experiments were recorded with use of the hypercomplex method of phase incrementation to obtain quadrature phase detection in ω_1.[40] The spectral width of ω_1 was the same as that in ω_2, which led to folding of the spectrum, and 2048 (for **1**) and 4096 (for **2**) complex points were collected and the total number of transients recorded were 8 and 16 (for **1**) and 4 and 8 (for **2**) for real and complex data, respectively. For all experiments, the value of Δ for the double quantum polarization transfer was set to 4.3 ms, corresponding to a maximum magnetization transfer for $^1J_{CC} = 57$ Hz that was the average of the sp^2-sp^2 one-bond coupling constants. Decoupling of ^{1}H during the entire experiment was performed by using the WALTZ scheme built into the spectrometer hardware. The total recycle delay (acquisition time plus relaxation delay) was set to 18 (for **1**) and 19.2 s (for **2**), which is approximately 0.90 (for **1**) and 0.96 (for **2**) times the average sp^2 ^{13}C spin−lattice relaxation time of 20 s.

Ab initio calculations were preformed with Gaussian98[41] on a HP Exemplar SPP-2200 computer at the University of Kentucky Computation Center, part of the National Computational Science Alliance. Ring currents were calculated with the finite field version of the London theory,[42] using the B3LYP 6-31G* structures with the resonance integrals set to the benzene value.

Acknowledgment. The authors thank the National Science Foundation (Grant CHE-9816339) for financial support of this project and Mr. W. John Layton for assistance with NMR measurements. This work was supported in part by the MRSEC Program of the National Science Foundation under Award No. DMR-9809686.

Supporting Information Available: Projections of **1** and **2** showing chemical shift assignments and $^{13}C-^{13}C$ coupling constants, and a table with the calculated and measured chemical shifts of **2** (PDF). This material is available free of charge via the Internet at http://pubs.acs.org.

JA012513R

(38) For examples of related systems with paramagnetic ring currents, see: (a) Kaplan, M. L.; Haddon, R. C.; Schilling, F. C.; Marshall, J. H.; Bramwell, F. B. *J. Am. Chem. Soc.* **1979**, *101*, 3306−3308. (b) Haddon, R. C.; Kaplan, M. L.; Marshall, J. H. *J. Am. Chem. Soc.* **1978**, *100*, 1235−1239.

(39) Delsuc, M. A.; Lallemand, J. Y. *J. Magn. Reson.* **1986**, *69*, 504−507.

(40) States, D. J.; Haberkorn, R. A.; Ruben, D. J. *J. Magn Reson.* **1982**, *48*, 286−292.

(41) Frisch, M. J.; Trucks, G. W.; Schlegel, H. B.; Scuseria, G. E.; Robb, M. A.; Cheeseman, J. R.; Zakrzewski, V. G.; Montgomery, J. A., Jr.; Stratmann, R. E.; Burant, J. C.; Dapprich, S.; Millam, J. M.; Daniels, A. D.; Kudin, K. N.; Strain, M. C.; Farkas, O.; Tomasi, J.; Barone, V.; Cossi, M.; Cammi, R.; Mennucci, B.; Pomelli, C.; Adamo, C.; Clifford, S.; Ochterski, J.; Petersson, G. A.; Ayala, P. Y.; Cui, Q.; Morokuma, K.; Malick, D. K.; Rabuck, A. D.; Raghavachari, K.; Foresman, J. B.; Cioslowski, J.; Ortiz, J. V.; Stefanov, B. B.; Liu, G.; Liashenko, A.; Piskorz, P.; Komaromi, I.; Gomperts, R.; Martin, R. L.; Fox, D. J.; Keith, T.; Al-Laham, M. A.; Peng, C. Y.; Nanayakkara, A.; Gonzalez, C.; Challacombe, M.; Gill, P. M. W.; B. Johnson, W. C.; Wong, M. W.; Andres, J. L.; Gonzalez, C.; Head-Gordon, M.; Replogle, E. S.; Pople, J. A.; *Gaussian98*; Gaussian, Inc.: Pittsburgh, PA, 1998.

(42) Pasquarello, A.; Schlüter, M.; Haddon, R. C. *Science* **1992**, *257*, 1660−1661.